Development of a Continuous Emulsion Copolymerization Process in a Tubular Reactor

Antonio C. S. M. Carvalho,[†] Dennis L. Chicoma,[†] Claudia Sayer,[‡] and Reinaldo Giudici*,[†]

Universidade de São Paulo, Escola Politécnica, Departamento de Engenharia Química, Caixa Postal 61548, CEP 05424-970, São Paulo, SP, Brasil, and Universidade Federal de Santa Catarina, CTC, Departamento de Engenharia Química e Alimentos, Caixa Postal 476, CEP 88040-970, Florianópolis, SC, Brasil

This contribution describes the development of a continuous emulsion copolymerization processs for vinyl acetate and *n*-butyl acrylate in a tubular reactor. Special features of this reactor include the use of oscillatory (pulsed) flow and internals (sieve plates) to prevent polymer fouling and promote good radial mixing, along with a controlled amount of axial mixing. The copolymer system studied (vinyl acetate and butyl acrylate) is strongly prone to composition drift due to very different reactivity ratios. An axially dispersed plug flow model, based on classical free radical copolymerization kinetics, was developed for this process and used successfully to optimize the lateral feeding profile to reduce compositional drift. An energy balance was included in the model equations to predict the effect of temperature variations on the process. The model predictions were validated with experimental data for monomer conversion, copolymer composition, average particle size, and temperature measured along the reactor length.

Introduction

Emulsion polymerization processes are widely used for the industrial production of different commercial products, such as paints, coatings, adhesives, and varnishes, that are typical applications of filming-forming latexes and can be carried out with a great variety of monomers in different types of reactors. Emulsion polymerization occurs in a heterogeneous medium composed of water as the continuous phase, emulsifiers, monomers, water-soluble initiator and additives. Because of the multiphase and compartmentalized nature, high molecular weights and high polymerization rates can be achieved, thus favoring higher productivity and lower residual monomer contents in the final latex composed of submicrometric polymer particles.

In a typical emulsion polymerization process, several phases may be present. The mixture of monomers are dispersed in water as droplets and stabilized by emulsifier in their surface. Excess of emulsifier may form micelles that are swollen by monomer. Radicals produced in the aqueous phase by decomposition of water-soluble initiator react with monomer forming oligoradicals. After grow some monomeric units, oligoradicals become hydrophobic enough to be able to enter into micelles, if present, thus producing polymer particles (micellar nucleation), or enter into previously formed polymer particles. The oligoradicals in the aqueous phase can further grow up to a critical length, at which they precipitate and, after being stabilized by emulsifier, form a new polymer particle (homogeneous nucleation). Mass transfer of monomers is generally much faster than the polymerization, so that the distribution of the monomers in the different phases (droplets, aqueous phase, monomer-swollen polymer particles, and monomer-swollen micelles) is assumed to be in equilibrium. Similarly, the distribution of emulsifier on the different surfaces (droplets, polymer particles, micelles) and dissolved in aqueous phase are considered in equilibrium. Monomer diffuses from the droplets to the polymer particles, which is the main locus of the polymerization process, following the classical mechanisms of free-radical polymerization (propagation, chain transfer, termination). Chain transfer to monomer generates small radicals that can exit the polymer particles to the aqueous phase. The full mechanism of emulsion polymerization is rather complex and is described in details in the literature;[33,36] only a short description of the process was presented.

Most of the industrial emulsion polymerization processes are carried out using batch or semibatch reactors, due to their flexibility and multiproduct features. The main drawback is related to control of the product quality due to the batch-to-batch variability. Continuous reactors present the advantages of lower volumes and better control of polymer quality, as they are typically operated under a steady-state regime. Continuous stirred tank reactors (CSTRs) may exhibit self-sustained periodical oscillations in monomer conversion and particle sizes under certain operating conditions. These oscillations can be minimized or avoided in tubular reactors with pulsed flow because of a lower level of backmixing; moreover, tubular reactors present further advantages over CSTRs, such as higher operational flexibility, less off-spec product because of shorter transients during startup, shutdown and grade transitions, and better temperature control because of the higher heat transfer area-to-volume ratio.[1] Tubular reactors can also be operated as loop reactors using high recyling rates, with the advantages of high heat transfer area and high flow velocity; however, loop reactors work essentially as a CSTR (in terms of backmixing) and thus are potentially prone to the occurrence of self-sustained oscillations under certain operating conditions.[2] An interesting alternative is the utilization of tubular reactors without recycle, along with pulsed (oscillatory) flow. More specifically, with reference to pulsed continuous tubular reactors, these actually can be of three types: pulsed column (PC),[3,4] pulsed packed column (PPC)[5,37−39] and pulsed sieve plate column (PSPC).[6,7] In all cases, pulsations produce sufficient turbulence to avoid clogging and fouling by the polymer particles. The presence of internals (packing or sieve plates) promotes appropriate flow patterns that favor radial mixing and thus reduce radial gradients of velocity, concentration and temperature. Recent publica-

* To whom correspondence should be addressed. Phone (55-11)30912254. Fax: (55-11)30912246. E-mail: rgiudici@usp.br.
[†] Universidade de São Paulo.
[‡] Universidade Federal de Santa Catarina.

10.1021/ie100422v
Published on Web 09/14/2010

Table 1. Formulation of the Continuous VAc−BuA Copolymerizations

reactants	weight fraction
water	0.8069
SLS	0.0024
$Na_2S_2O_8$	0.0029
VAc[a]	0.1596
BuA[a]	0.0282

[a] Initial proportion VAc/BuA = 0.85/0.15.

tions[6,8−10,40] studied emulsion homo- and copolymerizations in a PSPC and showed that the presence of sieve plates combined with pulses allowed one to minimize radial gradients of temperature and concentration, as well as, latex coagulation. In addition, the amplitude and frequency of the pulses may also be used to vary the axial dispersion along the column, which in turn may affect polymer properties.[3−5,11−13]

The aim of this work is to report the development of a continuous process for emulsion copolymerization of vinyl acetate (VAc) and butyl acrylate (BuA) performed in a PSPC type tubular reactor. This pair of comonomers was chosen in this study because of the commercial importance of this system for the water-borne coating industries and also because of the differences in the aqueous phase solubilities and in the reactivity ratios of these monomers.[14,15] Both differences between these monomers contribute to a large compositional drift with conversion, making the control of the copolymer composition throughout the reaction difficult, thus affecting the polymer chain microstruture and the thermal and mechanical properties of the polymer.[14,16,17] To improve its operational flexibility, the PSPC tubular reactor is composed of five sections, each one presenting independent lateral feed and temperature controls. In this case, the PSPC provides different operational feeding possibilities that allow control of the copolymer composition by feeding the more reactive monomer along the column. For this reason, in this study the effect of the number of lateral feed streams on the polymer properties was evaluated. Different numbers of lateral monomer feed streams distributed along the reactor length were employed in the experimental runs and the resulting differences in the uniformity of the copolymer composition were evaluated. The development and the optimization of the lateral feedings were supported by a mathematical model representative of the process. Based on the model simulations, an optimal feeding profile was calculated and experimentally applied in the PSPC, allowing the production of a more homogeneous copolymer. The results also permitted the validation of the mathematical model as a reliable tool for the prediction of experimental runs.

Experimental Procedures

Materials. The following reactants were used in the continuous emulsion copolymerizations: industrial grade vinyl acetate (VAc), butyl acrylate (BuA), and acrylic acid as monomers, sodium persulfate ($Na_2S_2O_8$) as water-soluble initiator, sodium lauryl sulfate (SLS) as emulsifier, and distilled and deionized water. The inhibitor hydroquinone was used to stop the reaction in the samples collected at different points along the reactor length. Table 1 describes the formulations used throughout the continuous reactions in the PSPC reactor, and the Table 2 includes the operational parameters of the reactions.

Pulsed Sieve Plate Column Reactor. The PSPC reactor consists of five vertically mounted stainless steel sections; each one is 1000 mm long with a 40 mm inner diameter. The perforated plates, also made of stainless steel, have 39 holes placed in a triangular arrangement, resulting in 22.7% of free area in each plate. Plate spacing between two consecutive plates is 50 mm, resulting in a reactor void fraction of 95.7%. Figure 1 presents schematically the experimental unit. A pulsator (G) is located at the bottom of the reactor, and its pulsation provides a combination of good local agitation with little backmixing, preventing deemulsification along the reactor and reactor clogging, and reducing radial gradients of temperature and concentration. The amplitude of pulses (stroke length) was 18 mm and the pulsation frequency was set to 2.1 Hz. In all sections, the same inlet cooling jacket temperature was kept constant, ranging from 56 to 57.5 °C, by controlled mixing of hot and cold water. Reactants are fed in the bottom of the reactor and flow upward. There are four additional lateral feeding points in the flanges between two consecutive sections. The flow rates of all monomer and aqueous phase feed streams were maintained constant by using a computer-based PI controller system. In this case, metering pumps (L) were controlled according to the weight decrease of the tanks (B and C) containing monomer and aqueous phase. The temperature of the water entering the

Table 2. Operational Conditions of the PSPC Reactor

operation variable	value
pulse amplitude	18 mm
Pulse frequency	2.1 Hz
jacket temperature	56 − 57.5 °C
average residence time	30 min
total reaction time	180 min

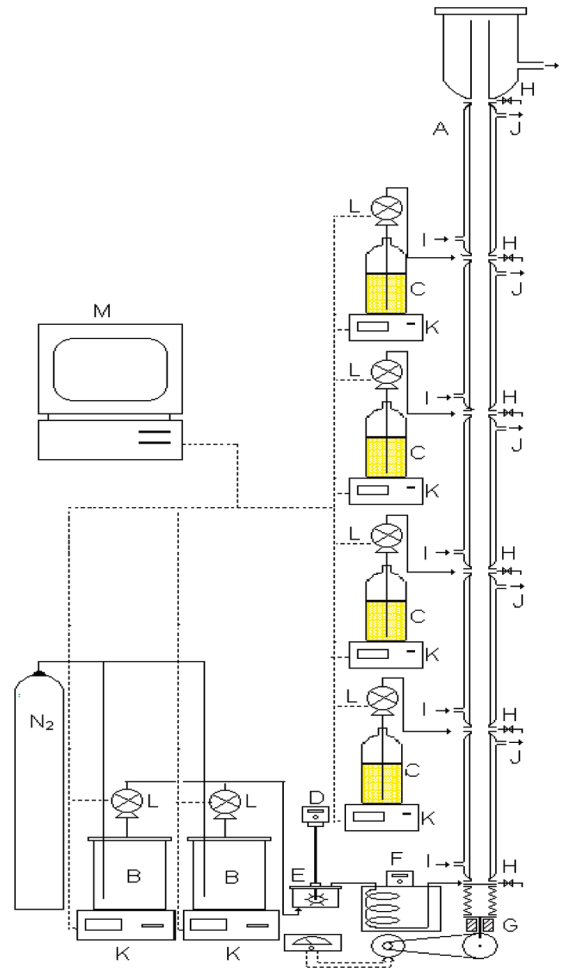

Figure 1. Continuous pulsed sieve plate column reactor. A, Reactor; B, C, feed tanks; D, agitator; E, premixing tank; F, heater; G, pulsator; H, sampling points; I, jacket entrance; J, jacket outlet; K, balances; L, metering pumps; M, computer. Internals (sieve plates) are not shown.

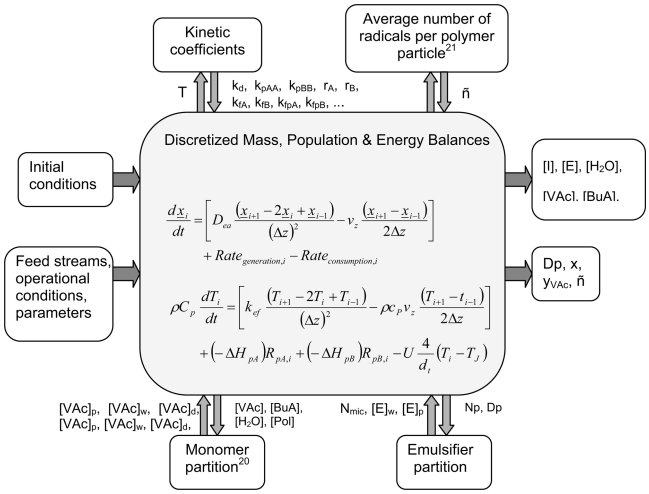

Figure 2. Simplified flow diagram of the mathematical model.

Table 3. Parameters Used in the Simulations (A = VAc, B = BuA)

parameter	value	units	source
k_d	1.8×10^{17} exp[−17155/T]	s^{-1}	Rawlings and Ray[24]
k_{pAA}	1.445×10^{10} exp[−2489.65/T]	cm³/mol s	Hutchinson et al.[25]
k_{pBB}	$2{,}73 \times 10^{9}$ exp[−3170/T]	cm³/mol s	McKenna et al.[26]
k_{pAB}	k_{pAA}/r_A	cm³/mol s	
k_{pBA}	k_{pBB}/r_B	cm³/mol s	
k_{fAA}	$2.43 \times 10^{-5}\ k_{pAA}$	cm³/mol s	Chatterjee et al.[27]
k_{fBB}	$1.9 \times 10^{-4}\ k_{pBB}$	cm³/mol s	Brandrup and Immergut[28]
k_{fAB}	k_{fAA}/r_A	cm³/mol s	
k_{fBA}	k_{fBB}/r_B	cm³/mol s	
k_{tAA}	5.255×10^{9} exp[−884/T]	cm³/mol s	Baad et al.[29]
k_{tBB}	1.6794×10^{7} exp[−1409/T]	cm³/mol s	McKenna et al.[26]
k_{tAB}	k_{tAA}	cm³/mol s	
r_m	2.5×10^{-7}	cm	Min and Ray[30]
$[E]_{CMC}$	2.43×10^{-6}	mol/cm³	Unzueta and Forcada[31]
D_{WA}	1.1×10^{-5}	cm²/s	Min and Ray[30]
D_{WB}	1.0×10^{-5}	cm²/s	Gardon[32]
D_{pA}	1.1×10^{-6}	cm²/s	Min and Ray[30]
D_{pB}	1.0×10^{-7}	cm²/s	Gardon[32]
f_{absA}	1.95×10^{-2}		adjusted
f_{absB}	5.9×10^{-5}		adjusted
f_{absmA}	0.15×10^{-5}		adjusted
f_{absmB}	1.0×10^{-8}		adjusted
c^0_{cA}	1.0×10^{-27}	s^{-1}	adjusted
c^0_{cB}	0.0	s^{-1}	Sayer and Giudici[19]
c^0_{homA}	3.0×10^{-3}	s^{-1}	Sayer and Giudici[19]
c^0_{homB}	1.0×10^{-5}	s^{-1}	Sayer and Giudici[19]
j_{critA}	16		Gilbert[33]
j_{critB}	8		Gilbert[33]
j_{zA}	8		Gilbert[33]
j_{zB}	1		Gilbert[33]
k^d_A	34.7		Gardon[32]
k^d_B	705.0		Unzueta and Forcada[31]
k^p_A	28.0		adjusted
k^p_B	460.0		Unzueta and Forcada[31]
r_A	0.04		Pichot et al.[34]
r_B	4.7		adjusted
a_s	$[39.3w_a + 26.5(1 - w_a)]$ $N_A \times 10^{-16}$	cm²/mol	adjusted
ΔH_A	−20895	cal/mol	Brandrup and Immergut[28]
ΔH_B	−15439	cal/mol	BASF[35]
C_p	1.0	cal/(g K)	adopted
Pe_m	61.6		Palma and Giudici[13]
Pe_h	7.0		adjusted
U_A	72	cal/(s K)	measured

jacket was controlled (PI controller) by the mixture of hot and cold water streams. Samples can be taken from the sampling valves located along the reactor length, at the end of each section of the reactor.

Table 4. Operational Conditions Used in the Experimental Run

		BuA feeding profile				
run	average jacket temperature (°C)	$z = 0$ m	$z = 1$ m	$z = 2$ m	$z = 3$ m	$z = 4$ m
A	57.5	100%				
B	57.3	33.33%	33.33%	33.33%		
C	57.5	33.33%		33.33%	33.33%	
D	56.5	25%	25%	25%	25%	
E	57.2	20%	20%	20%	20%	20%
F	56.0	13%	41%	27%	10.6%	8.4%

Latex Characterization. Monomer Concentrations. Residual VAc and BuA concentrations were determined by gas chromatography (Shimadzu HS-GC 17A with headspace sampling device) combined with gravimetry. *Conversion*: Monomer conversion (x) was calculated from gravimetric data. *Copolymer composition*: The cumulative composition of the copolymer (weight fraction of VAc in the copolymer) was calculated from monomer concentrations measured by gas chromatography. *Average particle diameter*: Photon correlation spectroscopy (Coulter N4-Plus) was used to measure the average particle diameters (D_p).

Particle Number Per Gram of Latex (Particle Concentration). Conversion and average particle diameter data were used to calculate the particle number (N_p).

Mathematical Model. The mathematical model for the emulsion copolymerization of VAc and BuA in a PSPC-type tubular reactor is based on the one-dimensional axially dispersed plug-flow model previously developed by our group.[18,19] In this model, the flow velocity is assumed to be the average net value (a constant value, without pulsation) and the axial mixing effect of the flow oscillations is accounted for by the axial dispersion term. In the present study, the energy balance was included in the model so that the influence of different temperature profiles could be taken into account.

With regard to the kinetic model for the copolymerization reactions, the classical free radical mechanism (considering initiator decomposition, initiation, propagation, transfer to monomer, transfer to polymer, and termination steps) was adopted, and the following assumptions were considered:

- Monomer concentrations in polymer particles, monomer droplets, and aqueous phase are at thermodynamic equilibrium and are computed using the iterative procedure proposed by Omi et al.[20] (1985).
- Total mass of polymer produced in the aqueous phase is negligible.
- Particle nucleation occurs through micellar and homogeneous mechanisms.
- Particle coagulation depends on initiator concentration.
- The average number of radicals per polymer particle is computed by using the method of continued fractions proposed by Ugelstad et al.[21] (1967).
- Polymer particles are spherical and monodisperse.
- The critical micellar concentration and the surface covered per mol of emulsifier are constant.
- The pseudo-steady-state assumption is valid for polymer radicals.
- Kinetic constants do not depend on the chain length.
- Kinetic constants in the aqueous and polymer phases are the same.
- Radicals generated by initiation or chain transfer to monomer and polymer have similar reactivities.
- The pseudokinetic (pseudohomopolymerization) approach is adopted for calculating the reaction rates of the copolymerization system.

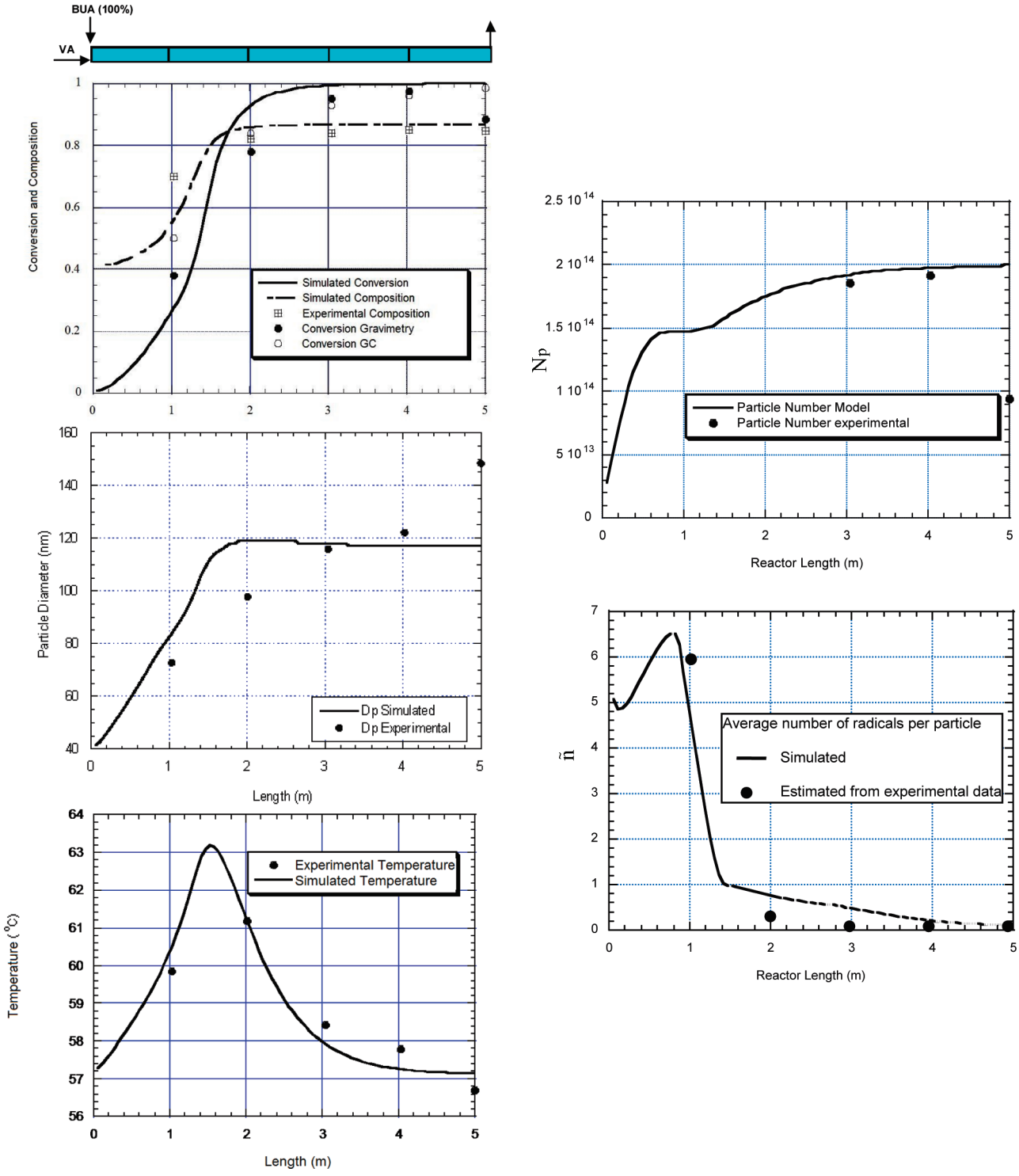

Figure 3. Evolution of the global conversion, copolymer composition, particle diameter, temperature, particle number and average number of radicals per particle during VAc−BuA copolymerization without lateral feed (run A).

Details of the kinetic model can be found in Sayer and Giudici[19] and, for the sake of conciseness, will not be repeated in detail here.

The mass balances are written for the polymer particles, initiator, emulsifier, water, polymer, and monomers A (vinyl acetate, VAc) and B (butyl acrylate, BuA) in a general form

$$\frac{\partial \underline{x}}{\partial t} + v_z \frac{\partial \underline{x}}{\partial z} - D_{ea} \frac{\partial^2 \underline{x}}{\partial z^2} = \text{rate}_{\text{generation}} - \text{rate}_{\text{consumption}} \tag{1}$$

with the Danckwerts[22] type boundary conditions

$$\underline{x}|_{z=0} = \underline{x}_{\text{feed}} + \frac{D_{ea}}{v_z} \frac{\partial \underline{x}}{\partial z}\bigg|_{z=0} \tag{2}$$

$$\frac{\partial \underline{x}}{\partial z}\bigg|_{z=L} = 0 \tag{3}$$

where $\underline{x}$ is the vector of the above-mentioned mass balance state variables, z is the axial position, t is time, L is the total reactor

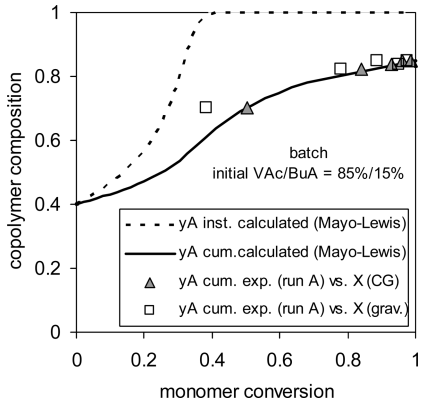

Figure 4. Plot of Mayo−Lewis equation for the copolymerization of VAc and BuA.

length, v_z is the net forward axial velocity of the fluid (= volumetric flow rate divided by the free cross sectional area), and D_{ea} is the effective axial dispersion coefficient.

The energy balance was implemented in the present work by using similar assumptions and is written as

$$\rho C_p \frac{\partial T}{\partial t} + \rho C_p v_z \frac{\partial T}{\partial z} - k_{ef} \frac{\partial^2 T}{\partial z^2} = \sum_{i=A,B} (-\Delta H_{p,i}) R_{p,i} - U \frac{4}{d_t}(T - T_J) \quad (4)$$

with the corresponding boundary conditions

$$T|_{z=0} = T_{feed} + \frac{k_{ef}}{\rho C_p v_z} \left.\frac{\partial T}{\partial z}\right|_{z=0} \quad (5)$$

$$\left.\frac{\partial T}{\partial z}\right|_{z=L} = 0 \quad (6)$$

where ρ and C_p are, respectively, the density and specific heat of the reaction medium, $\Delta H_{p,i}$ is the heat of polymerization of the monomer i (i = A,B), $R_{p,i}$ is the rate of polymerization of the monomer i, U is the global heat transfer coefficient between the reactor contents and the water flowing in the jacket, T and T_J are, respectively, the temperature of the reaction medium and the temperature of the water in the jacket, d_t is the reactor diameter, k_{ef} is the effective axial thermal conductivity.

The set of 8 partial differential equations given by the mass and heat balances was numerically solved by using the method of lines. The axial coordinate was discretized in ND nodes and the axial first and second derivatives were approximated by finite difference formulas. The resulting set of 8 × ND ordinary differential equations was then solved by using the DASSL solver.[23] All simulations reported were performed with ND = 90 axial discretization points; this number was determined from previous simulations to be sufficient to not affect the solution. The model can simulate the transient behavior of the process (e.g., startups, shutdowns, disturbances, transitions, etc.), as well as the steady state axial profiles of the variables (as a function of the axial position) as the responses of the model for very long times. Figure 2 illustrates the model structure.

Table 3 presents the set of parameters used in all simulations. Most of them (i.e., most of the kinetic parameters and physical properties) were determined from previous work in literature, and a few were adjusted as fitting parameters.

The value of the effective axial dispersion coefficient D_{ea} was calculated as a function of the amplitude and frequency of pulsation, flow velocity, and plate spacing from the empirical correlations given by Palma and Giudici.[13]

The value of the heat transfer coefficient U was experimentally determined in experiments without reaction for different values of the pulsation frequency (see Appendix).

The value of the effective axial thermal conductivity could be roughly estimated by assuming that mass and heat dispersion caused by the pulsations are analogous; under this hypothesis, the dimensionless groups axial mass Peclet number ($Pe_m = v_z L/D_e$) and the axial heat Peclet number ($Pe_h = \rho C_p v_z L/k_{ef}$) would be equal. However, the conduction through the reactor walls and internals imparts additional axial heat dispersion mechanisms, so that $Pe_h < Pe_m$. In the present work, Pe_h was estimated by fitting the model responses to the experimentally measured temperature profiles.

Results and Discussion

In this section, the results are present for six experimental runs that were carried out under steady-state conditions (parameters indicated in Table 2) using different distributions of more reactive monomer feedings. The choice of the experimental conditions used in the experiments was primarily driven by the previous simulations of Sayer and Giudici,[19] who studied different feeding profiles of the more reactive monomer (BuA) along the reactor as an way to reduce the drift of the copolymer composition. The present experiments were performed to validate those predictions.

In addition, to test the prediction capability of the energy balance included in the model equations, the experiments reported in the present work were done without control of the reactor temperature; only the temperature of the water entering the jackets was controlled, thus allowing the occurrence of temperature variations along the reactor length by the exothermic polymerization. In this way, these experiments provided data for the nonconstant axial temperature profile useful for checking the model predictions of the energy balance.

Small differences in the value of the jacket temperature in the different runs (56.5 ± 1 °C) occurred because of variations in the boiler that supplied warm water to the jackets. The values of the temperatures at the reactor bottom varied in the range of 54−56 °C throughout all the experimental runs. Table 4 presents the average temperature of the jacket and the feeding profiles of monomer BuA along the different reactor sections for each run. Figures 2−7 present the comparison between the experimental data (discrete points) and the simulation results (continuous curves).

Run A. Run A was performed without lateral feed of BuA. All the feed (both monomers, aqueous phase, initiator, and emulsifier) was made exclusively at the bottom of the column. Figure 3 shows the evolution of the global conversion and copolymer composition, the temperature, the average particle size; number of particles, and average number of radicals per particle throughout the column reactor. Comparison of the experimental data (symbols) with the simulated results (curves) is presented. The agreement is, in general, satisfactory. The polymerization reaches almost full monomer conversion within the first half of the reactor length, where the corresponding increasing of temperature occurs. A very strong variation in the copolymer composition is observed as a result of the very different reactivity ratios of the two monomers. The copolymer composition starts with about 40% VAc at $z = 0$, reaching the average composition of 85% VAc in the last half of the reactor length. It should be mentioned that the reported values of copolymer composition (experimental and simulated ones) are

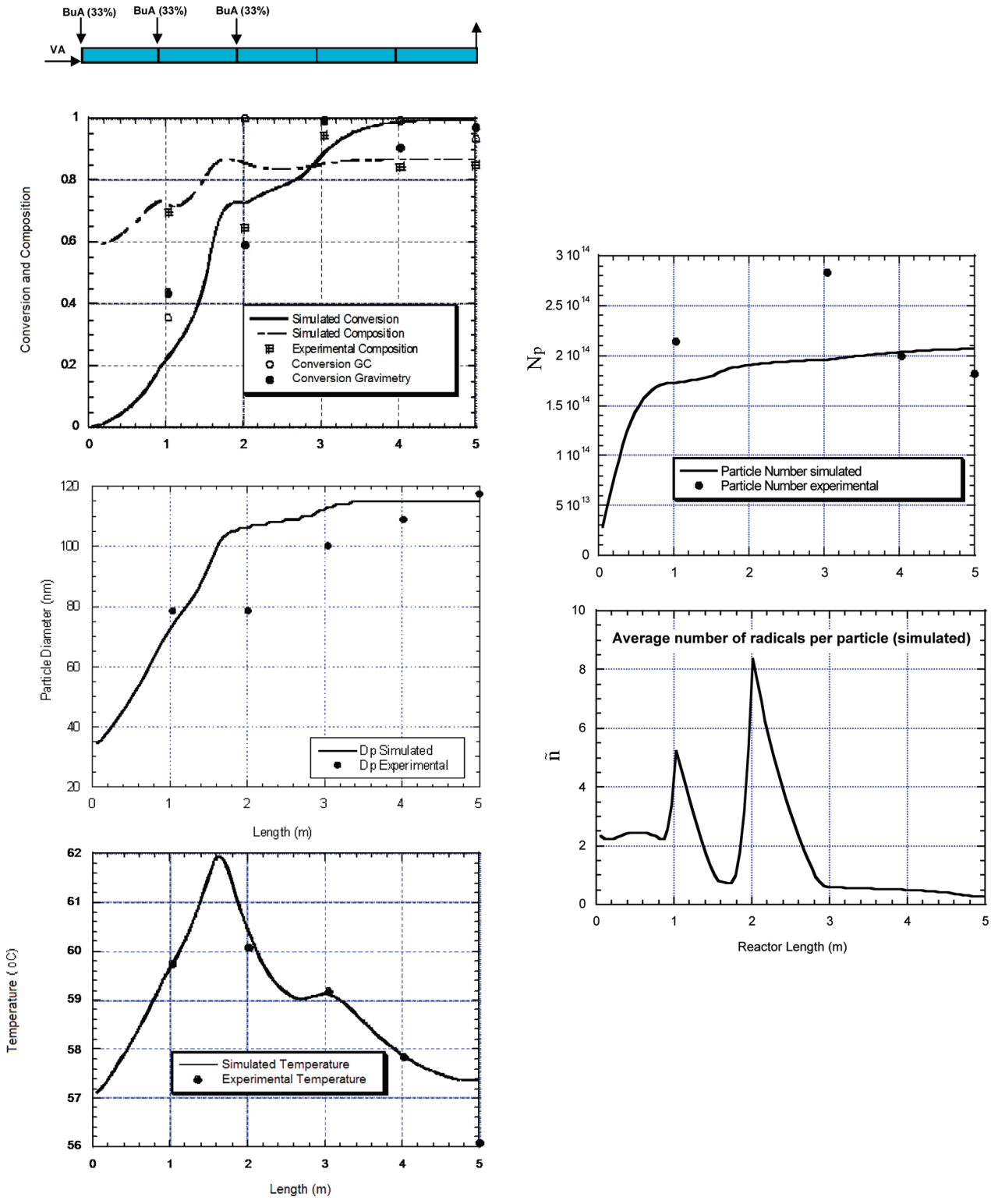

Figure 5. Evolution of the global conversion, copolymer composition, particle diameter, temperature, particle number, and average number of radicals per particle during VAc-BuA copolymerization with two BuA lateral feed at the end of sections 1 and 2 (run B).

cumulative values, for which the variations are damped. The instantaneous values of copolymer composition exhibit much stronger variations.

The values of average number of radicals per particle ($\tilde{n}$) are higher in the first section of the reactor, where BuA is polymerized. The system thus seems to follow a Smith−Ewart case III kinetics ($\tilde{n} > 1/2$) under the presence of BuA. After this comonomer is almost depleted (at the downstream 60% of the reactor length), the average number of radicals per particle decreases for very lower values, thus seeming to follow a Smith−Ewart case I kinetics ($\tilde{n} < 1/2$). This behavior is in agreement with the previous studies on VAc-BuA copolymerization in batch/semibatch tank reactors.[41,42] The "experimental" values of ñ can be roughly estimated from the monomer concentrations and the rate of polymerization (related to the slope of the conversion versus time curves), which is particularly difficult to obtain from our widely spaced data. The trend of $\tilde{n}$ is well described by the model.

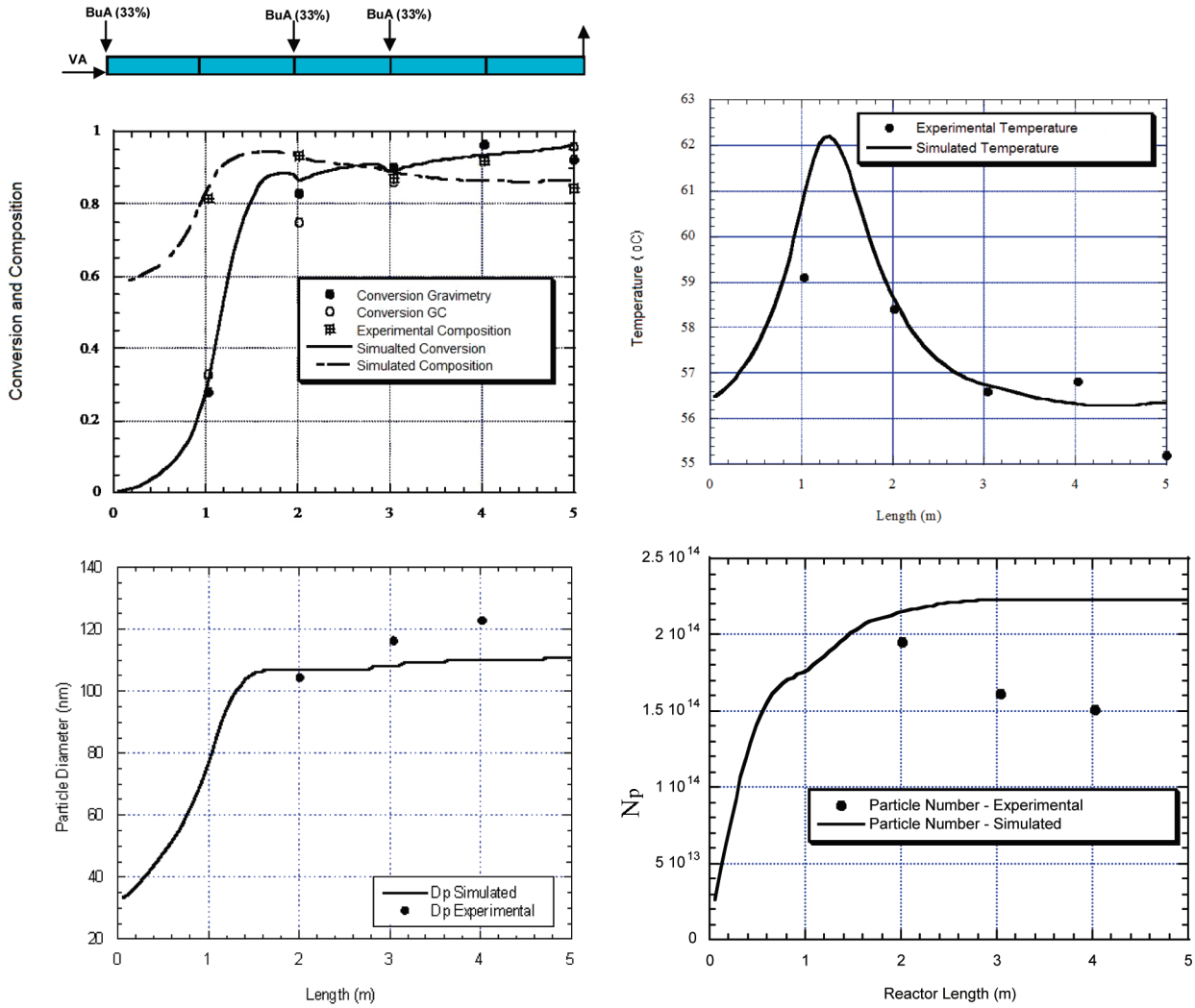

Figure 6. Evolution of the global conversion, copolymer composition, particle diameter, temperature, and particle number during VAc−BuA copolymerization with two BuA lateral feed at the end of sections 2 and 3 (run C).

Figure 4 presents the plot of the copolymer composition as a function of the total monomer conversion, calculated from the so-called Mayo−Lewis equation, using the reactivity ratios given in Table 3. The dashed line represents the instantaneous copolymer composition, i.e, the composition of the polymer produced at each conversion value. The continuous line represents the cumulative composition. This plot illustrates very clearly the problem of composition drift. For an initial mixture of monomers containing 85% VAc and 15% BuA, the composition of the first copolymer produced has 40% VAc and the polymer produced after about 40% conversion is almost 100% VAc (VAc homopolymer). The experimental data of run A (symbols) are also plotted in Figure 4, showing that the experimental values agreed very well with the Mayo−Lewis curve, especially for the conversion measured by GC.

Run B. Run B was carried out with the amount of BuA equally distributed in three points, the reactor bottom, and at the end of sections 1 and 2. Figure 5 shows the comparison of the experimental data with the model simulations. The distribution of the more reactive monomer in three points favors the reduction of the composition drift, in comparison to the case shown in Figure 3; however, there is still a large change in copolymer composition, stating from about 60% VAc at $z = 0$. The model predictions exhibit some oscillations in the conversion and composition profiles at $z = 1$ m and $z = 2$ m, the points of lateral feeding. The model follows reasonably the main trends of the variables. Larger differences between the model and experimental values for conversion and particle size were seen at the end of the first section ($z = 1$ m) and second section ($z = 2$ m) and can be ascribed to two reasons: (1) sampling at these points can be disturbed by the lateral feeding existing there and (2) at these points the rate of the polymerization reaction is very fast, so any delay in stopping the reaction in the sample can enhance the experimental error. The deviations in the experimental measurements performed in the tubular reactor are in general higher than in equivalent measurements made in batch/semibatch tank reactors. The difficulty is related to the sampling itself, especially because of the sampling points being located closer to the feeding points. Also, it is expected that disturbances caused by sampling are more severe in tubular reactors than in well-mixed tank reactor.

Large differences between model and experimental data are also observed for particle number (N_p), which is not a directly measured variable: actually, "experimental" values of N_p are calculated from the measurements of conversion (X) and particle size (D_p), so that the experimental errors in X and in D_p can be propagated in the calculation of N_p (moreover, N_p depends on the third power of D_p, so that even moderate errors in D_p may cause large errors in N_p). The simulated curve for the average number of radicals per particle confirmed that previously discussed trend: $\bar{n}$ is higher at regions closer to the BuA feeding

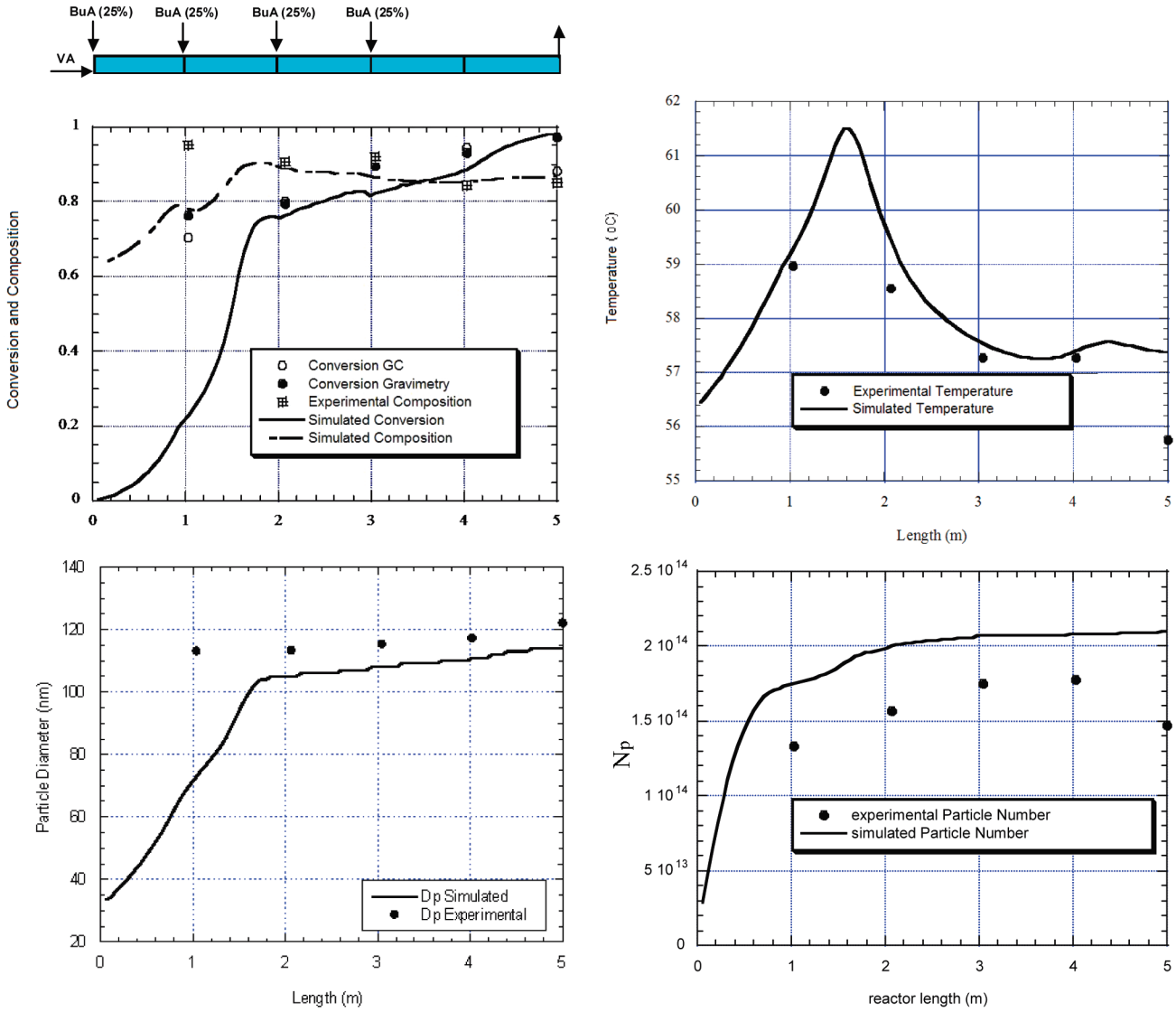

Figure 7. Evolution of the global conversion, copolymer composition, particle diameter, temperature and particle number during VAc−BuA copolymerization with three BuA lateral feeds at the end of sections 1, 2, and 3 (run D).

points, and much smaller at regions in which VAc polymerization is dominant.

Run C. Run C was carried out using two lateral feedings of BuA at $z = 2$ m and $z = 3$ m (at the end of sections 2 and 3), in addition to the feeding at the reactor bottom. The flow rate of BuA was equally divided into three fractions, with 33.33% of BuA being fed at the reactor bottom (together with the other reactants), 33.33% at $z = 2$ m and 33.33% at $z = 3$ m. Figure 6 shows that the simulation results again presented a good agreement with the experimental data throughout the sections of the tubular reactor. The results presented in this experiment, indicate that, because of the lateral feed streams of BuA in the central region of the reactor, an increase in the polymerization rate and temperature is observed in the first section because of the rapid consumption of BuA added at the base of the column.

Run D. Run D was carried out using 25% of BuA fed at the reactor bottom ($z = 0$) and three lateral feedings of 25% BuA at the end of sections 1, 2, and 3 ($z = 1$, 2, and 3 m). Figure 7 presents the comparison between experimental and simulated results. A small reduction in the composition drift can be observed with the increase in the number of lateral feedings, that is, when the more reactive monomer BuA is better distributed along the column is. As in the previous runs, a generally good agreement between the experimental data and the simulation results can be observed, with larger differences for the conversion and composition measured at the end of the first section, and for particle size and particle number, as already discussed. It can be observed that the lateral feeding of BuA causes a reduction in the polymerization reaction (indicated by the slope of the conversion versus length curves). Because of its higher reactivity ratio, the free radicals tend to react preferentially with BuA than with VAc, favoring the formation of BuA type radicals. On the other hand, the propagation rate constant of BuA homopolymerization is lower than the propagation rate constant of VAc homopolymerization. Therefore, a reduction in the overall polymerization rate is observed downstream from the lateral feeding points. Moreover, in the simulated curves, this rate reduction effect can be seen a little upstream of the lateral feeding point due to the effect of the axial dispersion.

Run E. In Run E, BuA was fed using four lateral feeds with equal amounts (20% in each stream) at the end of each section ($z = 1$, 2, 3, and 4 m), in addition to the main feeding at the reactor bottom ($z = 0$). The results are presented in Figure 8, showing a fair agreement between the simulation curves and the experimental data. This case presents the most distributed

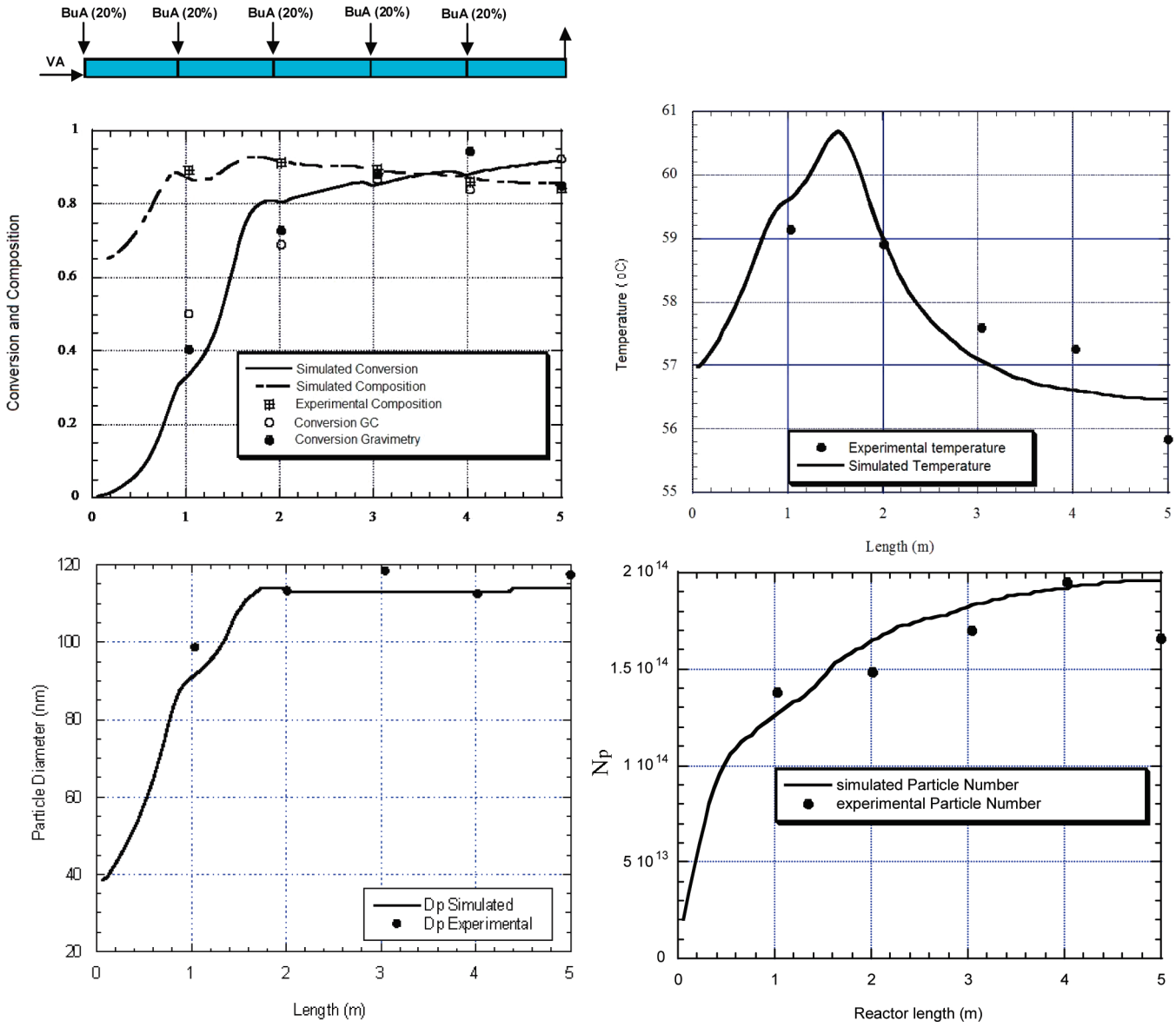

Figure 8. Evolution of the global conversion, copolymer composition, particle diameter, temperature and particle number during VAc-BuA copolymerization with four BuA lateral feeds at the end of sections 1, 2, 3, and 4 (run E).

feeding profile in comparison to the previous cases and, as a consequence, the copolymer composition was more uniform, as expected. Also, a smaller increase in the temperature was observed, reflecting a slightly lower polymerization rate profile along the reactor length. Therefore, a better control of temperature is achieved when the number of lateral feeding points is increased, an effect the can be ascribed in part to the effect of the cold feeding stream and in part to the effect of the lower propagation rate constant of BuA, as previously discussed.

Run F. It was noted in the previous cases that the increase of the number of lateral feeds with a more distributed profile of BuA favors a more uniform copolymer composition, as desired. However, this also causes an undesired reduction in the overall polymerization rate. In fact, this effect can be seen in the final monomer conversion at the reactor exit ($z = 5$ m); the final conversion for run E was 0.92, the lowest one among runs A−E. Moreover, even for run E, there are some important composition drifts in the first reactor section.

Run F presents an attempt to optimize the process. A conventional optimization approach was not tried due to the already heavy computational effort involved in the numerical solution of the model itself. Instead, a simplified approach to improve the feeding profile was devised, using ideas borrowed from process control. Additional equations of PID control were included in the model. The aim of this controller is to act on all feeding flow rates of the more reactive monomer (BuA). The controlled variables are the composition of the copolymer at the end of each reactor section. The equations for the controllers have the general form

$$\Delta F = k_c\left[(x_{sp} - x_{BuA}) + \frac{1}{\tau_I}\int (x_{sp} - x_{BuA})dt + \tau_\delta \frac{d(x_{sp} - x_{BuA})}{dt}\right] \quad (7)$$

where ΔF is the monomer feed variation in each step of the controller actuation for a specific column section; k_c is the controller proportional constant; τ_I, τ_δ are, respectively, the integral and derivative time constants; x_{BuA} and x_{sp} are, respectively, the computed BuA composition value in each actuation step at the sampling point (i.e., at the end of a specific reactor section) and its corresponding set point (the set point

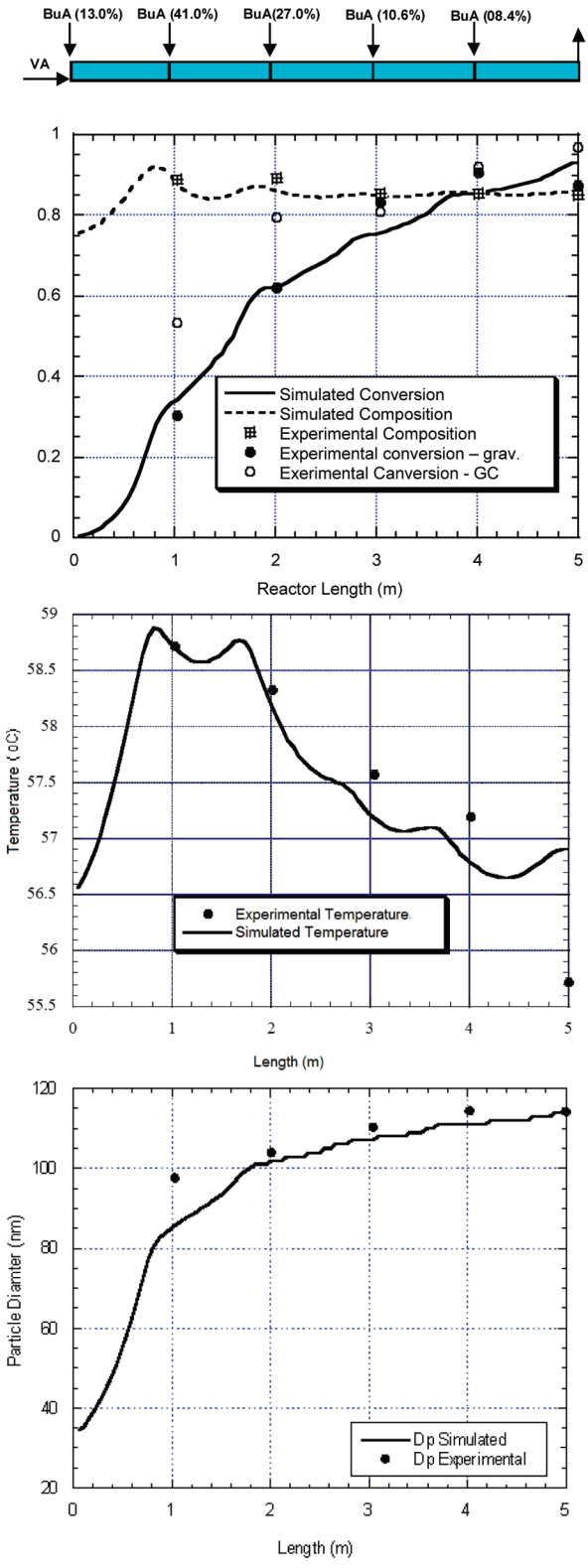

Figure 9. Evolution of the global conversion, copolymer composition, particle diameter and temperature during VAc-BuA copolymerization with four BuA "optimal" lateral feeds at the end of sections 1, 2, 3, and 4 (run F).

was $x_{sp} = 0.15$, which corresponds to a weight fraction of VAc of 0.85, the desired copolymer composition). An additional equation ensures that the sum of all BuA feed rates is equal to the total BuA feed rate established for the polymer formulation.

The adjusted feed rate values obtained by simulation of the model plus the controllers define the optimal feed rate profile along the column when the steady state of the simulated process and all established concentrations at the end of each section are achieved. This procedure forces a uniform copolymer composition along the column (particularly at the end of each section), but it does not guarantee complete monomer conversion at end of the column, which could be achieved by either reducing the average residence time of the fluid in the reactor (i.e., by changing the total flow rate), or changing the temperature profile (by acting on the jacket temperatures in each section of the reactor).

The "optimized" values of the BuA feeding distribution are those indicated in Figure 9, which shows the simulation and the corresponding experimental values obtained in run F, carried out using the "optimized" feeding profile. From the comparison between the runs C, E, and F, which were carried out at the same temperature in the cooling jacket, it can be observed that the final process conversion diminishes slightly with the homogeneity level achieved for the composition of the copolymer produced along the reactor at steady state conditions. Thus, there is a compromise between the established objectives for the conversion level and the desired homogeneity level of copolymer composition. Furthermore, it can be noted that the feed distribution of the more reactive monomer along the column is not only a control factor for the homogeneity of the obtained product but also an important operational variable that favors temperature control.

Under steady state conditions, with a constant cooling jacket temperature, the first two column sections are the regions of more intense variation in copolymer composition with axial position and with higher heat release by the polymerization. For this reason, the insertion of additional intermediate monomer feed points along these first two sections should give even better results.

Conclusions

A mathematical model for the emulsion copolymerization of VAc and BuA in a continuous tubular reactor (pulsed sieve plate column) was developed, improved, and validated with experimental data. The experimental values of temperature, monomer conversion, copolymer composition, and average particle size, measured under steady state conditions along the reactor length, agree satisfactorily with profiles obtained in the simulations, for different modes of lateral feeding. Thus, our model can predict with sufficient accuracy the effect of lateral monomer feed streams on the copolymer properties. The model can also take into account the influence of different temperature profiles, thus resulting in a powerful tool for process optimization.

Acknowledgment

The authors express their gratitude to CNPq (Conselho Nacional de Desenvolvimento Científico e Tecnológico) and FAPESP (Fundação de Amparo à Pesquisa do Estado de São Paulo) for their financial support, to Dow Brasil S.A. (Dow Latex -R&D), Rhodia Brasil Ltda. (Research Center of Paulínia) and BASF S.A. for providing monomers, to LCCA (Laboratório de Computação Científica Avançada) for providing computational resources, and to Prof. Frank Quina for revising the manuscript.

APPENDIX: Measurements of the Overall Heat Transfer Coefficient

Values for the overall heat transfer coefficients between the fluid inside the reactor and the water flowing in the jacket were

measured in experiments without polymerization, using water flowing inside the reactor. From the measurements of water flow rate inside the reactor ($\dot{m}$), inlet and outlet temperatures of the water inside the reactor (T_{in}, T_{out}), and the inlet and outlet temperatures of the water flowing in the jacket ($T_{J,in}$, $T_{J,out}$), in a cocurrent configuration of flow, the overall heat transfer coefficient can be estimated by

$$\dot{m}C_p(T_{in} - T_{out}) = UA\frac{(T_{in} - T_{J,in}) - (T_{out} - T_{J,out})}{\ln\left(\frac{T_{in} - T_{J,in}}{T_{out} - T_{J,out}}\right)} \quad (A.1)$$

The measurements were repeated for different pulsation frequencies, using the same flow rate as of that used in the polymerization runs. As an illustration of the results, the effect of the pulsation frequency on the measured overall heat transfer parameter UA is presented in Figure A.1. The assessment of the effect of fluid viscosity can be done by replacing the water by polymer emulsions of different viscosities.

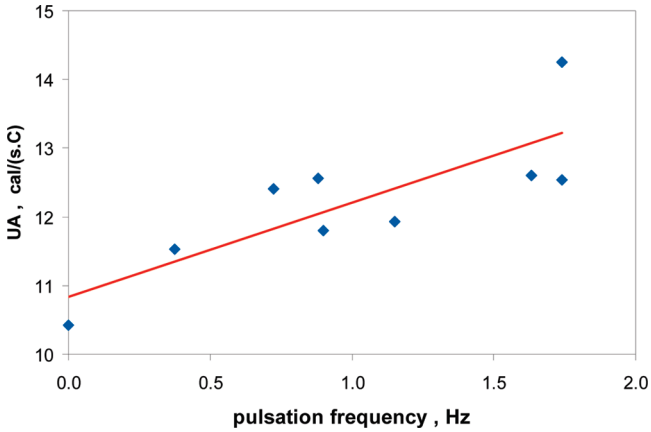

Figure A.1. Effect of the pulsation frequency on the heat transfer parameter, for water flowing inside the reactor.

Literature Cited

(1) Sayer, C.; Giudici, R. A Comparison of Different Modeling Approaches for the Simulation of the Transient and Steady-State behavior of Continuous Emulsion Polymerizations in Pulsed Tubular Reactors. *Braz. J. Chem. Eng.* **2002**, *19*, 89.

(2) Araújo, P. H. H.; de la Cal, J. C.; Asua, J. M.; Pinto, J. C. Modeling Particle Size Distribution (PSD) in Emulsion Copolymerization Reactions in a continuous Loop Reactor. *Macromol. Theory Simul.* **2001**, *10*, 769–779.

(3) Paquet, D. A., Jr.; Ray, W. H. Tubular Reactor for Emulsion Polymerization: I. Experimental Investigation. *AIChE J.* **1994**, *40*, 73.

(4) Paquet, D. A., Jr.; Ray, W. H. Tubular Reactor for Emulsion Polymerization: II. Model Comparisons with Experiments. *AIChE J.* **1994**, *40*, 88.

(5) Hoedemakers, G. F. M. Continuous Emulsion Polymerization in a Pulsed Packed Column. Ph. D. Thesis, Eindhoven University of Technology, Eindhoven, The Netherlands, 1990.

(6) Palma, M.; Sayer, C.; Giudici, R. A New Continuous Reactor for Emulsion Polymerization: Effect of Operational Conditions on Conversion and Particle Number. *Dechema Monogr.* **2001**, *37*, 625.

(7) Scholtens, C. A.; Meuldijk, J.; Drinkenburg, A. A. H. Production of Copolymers with a Predefined Intermolecular Chemical Composition Distribution by Emulsion Polymerization in a Continuously Operator Reactor. *Chem. Eng. Sci.* **2001**, *56*, 955.

(8) Palma, M.; Miranda, S.; Sayer, C.; Giudici, R. Comparação entre reações continuas de polimerização em emulsão em uma coluna pulsada com pratos perfurados com reações em batelada. Presented at the 6th CBPOL Congresso Brasilero de Polímeros, Gramado, Brazil, 2001.

(9) Sallarés, A. C.; Sayer, C.; Giudici, R. Copolymer Composition Control during Vinyl Acetate−Butyl Acrylate Emulsion Polymerization Reactions in a Continuous Pulsed Sieve Plate Column Reactor. *Dechema Monographs* **2004**, *138*, 323.

(10) Carvalho, A. C. S. M.; Chicoma, D.; Sayer, C.; Giudici, R. Comparison of Vinyl Acetate−Butyl Acrylate Emulsion Copolymerization Conduced in a Continuous Pulsed Sieve Plate Column Reactor and in a Batch Stirred Tank Reactor. *Macromol. Symp.* **2006**, *243*, 147.

(11) Meuldijk, J.; Van Strein, C. J. G.; Van Doormalen, F. A. H. C.; Thoenes, D. A Novel Reactor for Continuous Emulsion Polymerisation. *Chem. Eng. Sci.* **1992**, *47*, 2603.

(12) Scholtens, C. A. Process development for continuous emulsion. Ph. D. Thesis, Eindhoven University of Technology, Eindhoven, The Netherlands, 2002.

(13) Palma, M.; Giudici, R. Analysis of Axial Dispersion in an Oscillatory-Flow Continuous Reactor. *Chem. Eng. J.* **2003**, *94*, 189.

(14) Gugliotta, L. M.; Arotçarena, M.; Leiza, J. R.; Asua, J. M. Estimation of Conversion and Copolymer Composition in Semicontinuous Emulsion Polymerization Using Calorimetric Data. *Polymer* **1995**, *36*, 2019.

(15) Dimitratos, J.; Georgakis, C.; El-Aasser, M. S.; Klein, A. Pseudosteady States in Semicontinuous Emulsion Copolymerization. *J. Appl. Polym. Sci.* **1989**, *40*, 1005.

(16) Guillot, J. Modeling and Simulation of Emulsion Copolymerization of Monomers of Different Polarities - Relationship Polymerization Process−Microstructure−Properties. *Makromol. Chem. Macromol. Symp.* **1990**, *35/36*, 269.

(17) Chicoma, D.; Giudici, R.; Sayer, C. Efeitos da Composição de VAc-BuA através de Adições Intermitentes de BuA em uma Copolimerização em Emulsão Realizadas em Batelada. Presented at XVI COBEQ Congresso Brasileiro de Engenharia Química, Brazil, 2006.

(18) Sayer, C.; Palma, M.; Giudici, R. Modeling Continuous Vinyl Acetate Emulsion Polymerization Reactions in a Pulsed Sieve Plate Column. *Ind. Eng. Chem. Res.* **2002**, *41*, 1733–1744.

(19) Sayer, C.; Giudici, R. Simulation of Emulsion Copolimerization Reactions in a Continuous Sieve Plate Column Reactor. *Braz. J. Chem. Eng.* **2004**, *21*, 459.

(20) Omi, S.; Kushibiki, K.; Negishi, M.; Iso, M. Generalized Computer Modeling of Semi-Batch,n-Component Emulsion Copolymerization Systems and Its Applications. *Zairyo Gijutsu* **1985**, *3*, 426.

(21) Ugelstad, J.; Moek, P. C.; Aasen, J. O. Kinetics of Emulsion Polymerization. *J. Polym. Sci.* **1967**, *5*, 2281–2287.

(22) Dankckwerts, P. V. Continuous Flow Systems. Distribution of Residence Times. *Chem. Eng. Sci.* **1953**, 1.

(23) Petzold, L. R. *A Description of DASSL: A Differential Algebraic System Solver*; Sandia National Laboratories: Livermore, CA, 1982.

(24) Rawlings, J. B.; Ray, W. R. The Modelling of Batch and Continuous Emulsion Polymerization Reactors: II. Comparison with Experimental Data from Continuous Stirred Tank Reactors. *Polym. Eng. Sci.* **1988**, *28*, 257–274.

(25) Hutchinson, R. A.; Paquet, D. A.; McMinn, J. H.; Beuermann, S.; Fuller, R. E.; Jackson, C. *Dechema Monogr.* **1995**, *131*, 467.

(26) McKenna, T. F.; Graillat, C.; Guillot, J. Contributions to Defining the Rate Constants for the Copolymerization of Butyl Acrylate and Vinyl Acetate. *Polym. Bul.* **1995**, *34*, 361–368.

(27) Chatterjee, A.; Park, W. S.; Graessley, W. W. Free Radical Polymerization with Long Chain Branching: Continuous Polymerization of Vinyl Acetate in *t*-Butanol. *Chem. Eng. Sci.* **1977**, *32*, 167–178.

(28) Brandrup, J. Immergut, E. H. *Polymer Handbook*, 3rd ed.; Wiley: New York, 1989.

(29) Baad, W.; Moritz, H. U.; Reichert, K. H. Kinetics of High Conversion Polymerization of Vinyl Acetate Effects of Mixing and Reactor Type on Polymer Properties. *J. Appl. Polym. Sci.* **1982**, *27*, 2249–2268.

(30) Min, K. W.; Ray, W. H. The Computer Simulation of Batch Emulsion Polymerization Reactors Through a Detailed Mathematical Model. *J. Appl. Polym. Sci.* **1978**, *22*, 89–112.

(31) Unzueta, E.; Forcada, J. Modeling the Effect of Mixed Emulsifier Systems in Emulsion Copolymerization. *J. Appl. Polym. Sci.* **1997**, *66*, 445–458.

(32) Gardon, J. L. Emulsion Polymerization. II. Review of Experimental Data in the Context of the Revised Smith-Ewart Theory. *J. Polym. Sci., Part A* **1968**, *6*, 643–664.

(33) Gilbert, R. G. *Emulsion Polymerization. A Mechanistic Approach*; Academic Press: San Diego, CA, 1995.

(34) Pichot, C.; Llauro, M.-F.; Pham, Q.-T. Microstructure of Vinyl Acetate−Butyl Acrylate Copolymers Studied by ^{13}C-NMR Spectroscopy: Influence of Emulsion Polymerization Process. *J. Polym. Sci., Polym. Chem.* **1981**, *19*, 2619–2633.

(35) BASF S/A, *Acrilato de butila - Folheto Técnico*, edição 1, 2003, 2p.

(36) Asua, J. M. Emulsion Polymerization: From Fundamental Mechanisms to Process Developments. *J. Polym. Sci. A: Polym. Chem.* **2004**, *42*, 1025.

(37) Van den Boomen, F. H. A. M.; Meuldijk, J.; Thoenes, D. Emulsion Copolymerisation in a Flexible Continuously Operated Reactor. *Chem. Eng. Sci.* **1999**, *54*, 3283.

(38) Mayer, M. J. J.; Meuldijk, J.; Thoenes, D. Application of the Plug Flow with Axial Dispersion Model for Continuous Emulsion Polymerization in a Pulsed Packed Column. *Chem. Eng. Sci.* **1996**, *51*, 3441.

(39) Mayer, M. J. J.; Meuldijk, J.; Thoenes, D. Emulsion Polymerization in Various Reactor Types: Recipes with High Monomer Contents. *Chem. Eng. Sci.* **1994**, *49*, 4971.

(40) Sayer, C.; Palma, M.; Giudici, R. Modeling Continuous Vinyl Acetate Emulsion Polymerization Reactions in a Pulsed Sieve Plate Column. *Ind. Eng. Chem. Res.* **2002**, *41*, 1733.

(41) Saldivar, E.; Araujo, O.; Giudici, R.; Guerrero-Sanchez, C. Modeling and Experimental Studies of Emulsion Copolymerization Systems. III. Acrylics. *J. Appl. Polym. Sci.* **2002**, *84*, 1320.

(42) Kong, X. Z.; Pichot, C.; Guillot, J. Kinetics Of Emulsion Copolymerization Of Vinyl Acetate With Butyl Acrylate. *Eur. Polym. J.* **1988**, *24*, 485.

Received for review February 25, 2010
Revised manuscript received August 1, 2010
Accepted August 25, 2010

IE100422V